C−H Activation on Co,O Sites: Isolated Surface Sites versus Molecular Analogs

Deven P. Estes,[†] Georges Siddiqi,[†] Florian Allouche,[†] Kirill V. Kovtunov,[§,‖] Olga V. Safonova,[‡] Alexander L. Trigub,[⊥] Igor V. Koptyug,[§,‖] and Christophe Copéret*,[†]

[†]Department of Chemistry and Applied Biosciences, Eidgenössische Technische Hochschule Zürich, CH-8093 Zürich, Switzerland
[‡]General Energy Research Department, Paul Scherrer Institute, CH-5232 Villigen, Switzerland
[§]International Tomography Center, SB RAS, 3A Institutskaya St., Novosibirsk 630090, Russia
[‖]Novosibirsk State University, Pirogova St. 2, Novosibirsk 630090, Russia
[⊥]National Research Centre "Kurchatov Institute", 1 Akademika Kurchatova Pl., 123182 Moscow, Russia

Ⓢ Supporting Information

ABSTRACT: The activation and conversion of hydrocarbons is one of the most important challenges in chemistry. Transition-metal ions (V, Cr, Fe, Co, etc.) isolated on silica surfaces are known to catalyze such processes. The mechanisms of these processes are currently unknown but are thought to involve C−H activation as the rate-determining step. Here, we synthesize well-defined Co(II) ions on a silica surface using a metal siloxide precursor followed by thermal treatment under vacuum at 500 °C. We show that these isolated Co(II) sites are catalysts for a number of hydrocarbon conversion reactions, such as the dehydrogenation of propane, the hydrogenation of propene, and the trimerization of terminal alkynes. We then investigate the mechanisms of these processes using kinetics, kinetic isotope effects, isotopic labeling experiments, parahydrogen induced polarization (PHIP) NMR, and comparison with a molecular analog. The data are consistent with all of these reactions occurring by a common mechanism, involving heterolytic C−H or H−H activation via a 1,2 addition across a Co−O bond.
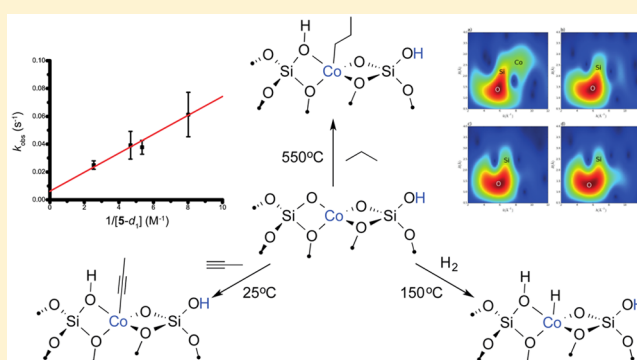
INTRODUCTION

Conversion of hydrocarbons from petroleum typically requires C−H activation before any changes to the carbon skeleton can take place. C−H activation processes are mediated by various heterogeneous catalysts including zeolites, supported metal nanoparticles, and isolated metal ions on oxide surfaces.[1] For example, the dehydrogenation of propane into propene and hydrogen is catalyzed by isolated metal sites on metal oxide supports[2] as well as well-defined homogeneous complexes through a mechanism involving C−H activation.[3] This process has regained momentum because of the abundance of low-cost propane and ethane from shale gas combined with the high demand for ethylene and propylene.[2d,4]

Propane dehydrogenation can be catalyzed by a variety of dispersed metal ions on silica, prepared by impregnation of metal salts on a support followed by calcination. In particular, in the case of Co(II) sites,[4b] the catalyst is very stable and its activity increases slightly with time on stream, unlike the industrial catalyst. They also observed that this catalyst gave excellent selectivity for propene (>95%) with very little cracking (ethylene and methane) or coking (C(s)), making this an excellent candidate for further investigations. The mechanism of propane dehydrogenation is thought to involve C−H activation by 1,2 addition across

a M−O bond (Figure 1),[1a] similar to molecular alkoxide and amide complexes.[5] This step is probably rate determining.
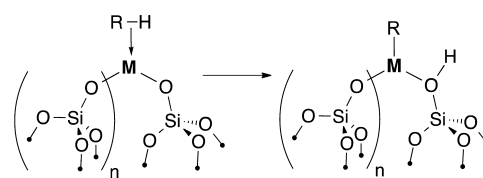
Figure 1. C−H activation on isolated surface ions.

However, direct experimental evidence for these types of C−H activations by isolated metal ions on surfaces is still lacking, owing to the difficulty of studying heterogeneous catalysts. Both the detection of reaction intermediates and kinetic measurements, a critical part of any mechanistic investigation,[6] are more difficult on surfaces than in solution. For instance, reactions on surfaces are often zero order in substrates due to either (1) strong substrate binding or (2) diffusion control (mass transport
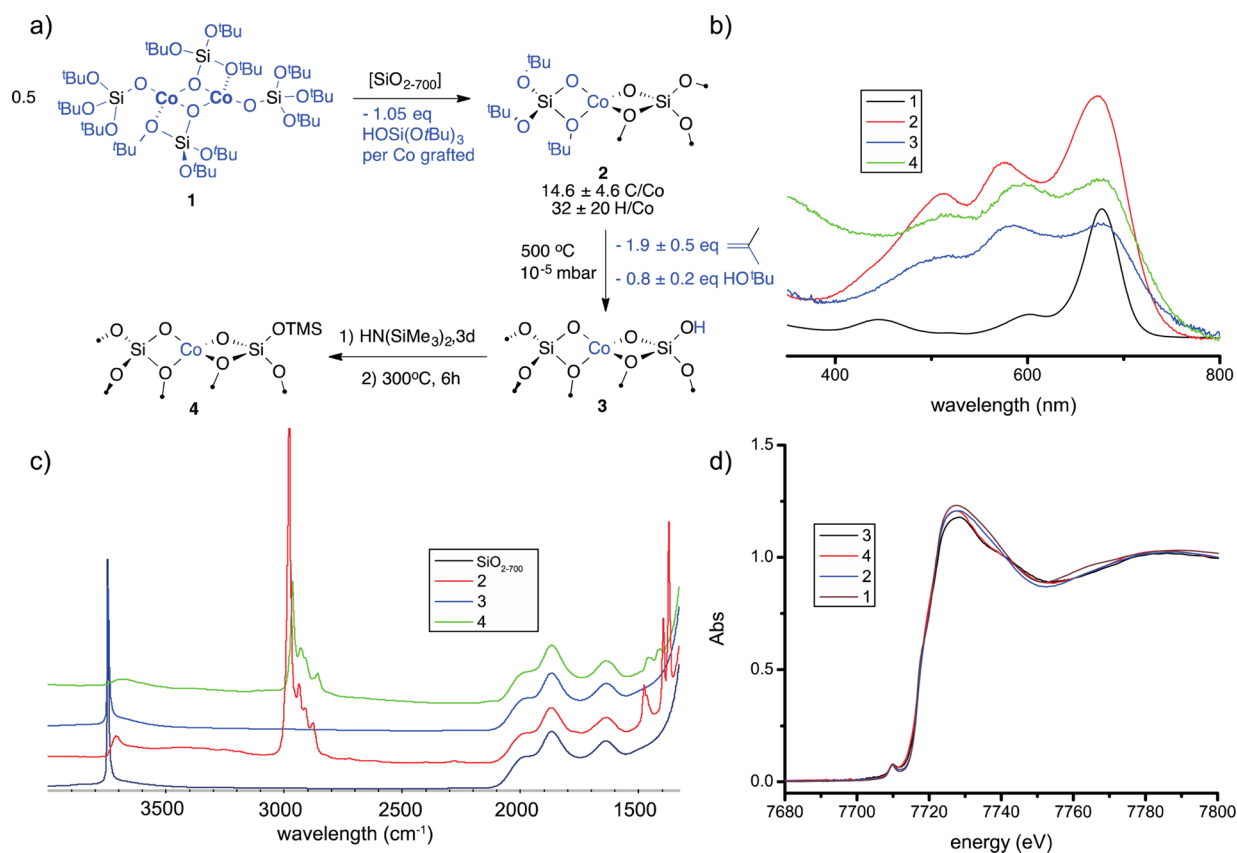
Figure 2. (a) Synthesis of grafted species on SiO_{2-700} and (b) UV−vis spectra, (c) IR spectra, and (d) XANES spectra of **1**, **2**, **3**, and **4**.

problems), precluding the measurement of a chemical rate law.[7] Kinetic measurements on surfaces are also complicated by factors such as heat transport within the catalyst and particle grain size,[7] making them much more difficult to quantify and often less informative than kinetics in solution. Moreover, surface sites are by and large ill-defined resulting in a distribution of activities.

Thus, one approach to circumvent the problem is to study the reactivity of well-defined surface species, prepared via a molecular approach.[8] Transition metal siloxides are known to be good molecular analogs of metal silicate surface sites.[8b,9] We recently used surface organometallic chemistry (SOM-C)[10a,9a,10b−e] combined with the thermolytic precursor approach (TPA)[11a,9a,11b,c] to synthesize isolated Cr(III) ions on a silica surface as well-defined analogues of industrial ethylene polymerization and propane dehydrogenation catalysts.[12] We also developed isolated W(VI) sites, which are highly active in metathesis at room temperature upon activation with an organosilicon agent.[13] This molecular level understanding of the structure of the surface sites and their reactivity provided new insights into these catalysts.

Here we use this strategy to synthesize well-defined isolated Co(II) sites on silica as shown by in depth characterization by IR, UV−vis, and XAFS. Detailed mechanistic investigations on molecular and surface entities indicate that heterolytic C−H and H−H bond activation processes across the M−O bond are involved in dehydrogenation, hydrogenation, and alkyne trimerization catalyzed by Co(II) surface species.

■ RESULTS

Synthesis and Characterization of Co(II) Surface Species. $Co_2(OSi(OtBu)_3)_4$ (**1**) was synthesized by reacting $Co(HMDS)_2(THF)$ with 2 equiv of $HOSi(OtBu)_3$ (synthesis and characterization details in the SI). This synthesis is analogous to that of $Co(4,4'\text{-ditBu-bipy})(OSi(OtBu)_3)_2$ that was previously reported by Tilley.[11b] When **1** is grafted onto SiO_{2-700} (0.32 mmol of OH g^{-1} corresponding a density of 0.9 OH nm^{-2}), it liberates 1 equiv of $HOSi(OtBu)_3$ per Co (0.29 mmol of $HOSi(OtBu)_3$ $g_{SiO_2}^{-1}$) to produce the light blue solid **2** containing 0.28 mmol of Co·g^{-1} (Figure 2a). The IR spectrum of **2** shows complete consumption of isolated silanols along with new bands between 2985 and 2870 corresponding to C−H stretching modes. The presence of a broad band at 3390 cm^{-1} indicates the presence of residual OH interacting with organic ligands. In addition, material **2** contains 14.6 equiv of C per Co and 32 equiv of H per Co according to elemental analysis (within experimental error of 1 equiv of $HOSi(OtBu)_3$ per Co). Treatment of **2** under high vacuum at 500 °C produces a total of 2.7 ± 0.7 equiv of isobutene and $tBuOH$ per Co, along with reformation of 0.55 mmol of SiOH groups g^{-1} and loss of the hydrocarbon groups (IR spectra, Figure 2c). We also prepared a material where the surface hydroxyls in **3** were replaced with $OSiMe_3$ groups by reaction with $HN(SiMe_3)_2$ (HMDS), yielding $Co@SiO_2-TMS$ (**4**) (see ESI for details). After this treatment, IR spectroscopy and elemental analysis showed that nearly all of the surface hydroxyls had been passivated (0.49 mmol of $SiMe_3$ g^{-1}) (Figure 2c).

All these data suggest that the surface species are monomeric Co centers, instead of dimeric as in the molecular precursor **1**. Similar to what we observe for Co, monomeric Zn(II) sites also form during the grafting of $Zn_2(OSi(OtBu)_3)_4$ onto SiO_{2-700}.[14] However, this is in contrast to what is observed when $Cr_2(OSi(OtBu)_3)_4$ is grafted on SiO_{2-700}.[12a] This difference may be attributed to the fact that later metals have higher d electron counts,

favoring lower coordination number and monomeric complexes. We decided to further interrogate the surface structure in order to confirm that the surface species formed in **3** was indeed a monomer.

Absorption of CO onto **3** produced an IR spectrum with only one blue-shifted peak at 2184 cm^{-1}. Blue shifted CO stretching frequencies are typical of first row transition metal ions on silica surfaces and zeolites[15,12b] and suggest that these metals ions are poor π donors and that bonding is dominated by electrostatic interactions.[16] The presence of only one peak suggests that the surface species are of uniform composition. In contrast, **1** and **2** do not adsorb CO, indicating a difference in the coordination environment in **3** vs **1** or **2**, caused by loss of the bulky (tBuO)$_3$SiO ligands during the thermal treatment. Species **1**, **2**, and **3** are EPR silent even at 4 K. Comparison of the UV−vis spectra of the starting molecular complex **1**, grafted material **2**, and thermally treated material **3** shows differences between molecular and surface species (Figure 2b). The molecular complex **1** displays one intense band at 677 nm with two of lower intensity at 602 and 448 nm, which is typical for dimeric four-coordinate Co(II) complexes.[17] However, **2** and **3** have spectra consisting of three bands of roughly equal intensity between 680 and 530 nm. This is similar to what is observed for monomeric pseudotetrahedral complexes like Na[Co(OH)$_3$(H$_2$O)][18] and Co(II)-exchanged zeolites.[19]

The XANES of **1**, **2**, **3**, and **4** display pre-edge features at ca. 7709.9 eV and the edge at ca. 7726 eV (Figure 2d), similar to that of Co(OAc)$_2$ and Co(acac)$_2$.[4b] The retention of the edge position during grafting and thermal treatment indicates a preservation of the Co(II) oxidation state, and the retention of the pre-edge feature indicates that the general symmetry of **1** is similarly maintained.

The EXAFS data were simulated to understand the coordination environment of cobalt. Table 1 shows the type and number of neighboring atoms in the fitting model as well as bond lengths and Debye−Waller factors. In all the complexes (**1−4**), we could fit the EXAFS data using four Co−O scattering paths. After thermal treatment, all Co−O bond lengths can be fit to the same average distance. The model used to fit the EXAFS data of molecular species **1** contained four nonequivalent Co−O paths based on its crystal structure. The two shorter Co−O paths correspond to the X type siloxide ligands, whereas the two longer ones are attributed to the L-type κ^2-siloxide interaction. For grafted species **2**, we obtained a good fit using two independent Co−O paths, while for **3** and **4**, adequate fits were possible using four equivalent oxygen neighbors. The increase in the Debye−Waller factors upon grafting and thermal treatment suggests that a wide distribution of geometries is present on the silica-supported species, consistent with the amorphous nature of silica. Based on its known crystallographic structure, we fit the second coordination shell of complex **1** using three Co−Si neighbors and one Co−Co neighbor. The EXAFS of the surface species **2**, **3**, and **4** also showed several scattering paths in the second coordination sphere. However, standard EXAFS simulation could not unequivocally determine whether a Co−Co path was present. In order to check for the presence of Co−Co paths, we performed a wavelet analysis of the EXAFS data of all of these complexes (Figure 3).[20] This analysis clearly demonstrates that a Co−Co scattering path is present in **1**, but only Co−Si paths are present in **2**, **3**, and **4**. This indicates that grafting **1** on the silica surface breaks the dimeric molecular complex up into monomers on the surface similar to what occurs for the Zn(II) analogues.[14]

Table 1. Fitting Parameters Obtained from Simulation of the EXAFS Spectra of 1, 2, 3, and 4

	neighbor	number	r (Å)	σ^2 (Å^2)
1[a]	O	1	1.84(4)	
		1	1.96(1)	
		1	2.05(4)	
		1	2.13(4)	
	Si	1	2.78(4)	
	Co	1	2.95(4)	
1[b]	O	1	1.83(7)	0.006(6)
		1	1.90(7)	0.006(6)
		1	1.99(4)	0.006(6)
		1	2.09(4)	0.006(6)
	Si	1	2.77(2)	0.0094(8)
	Co	1	2.92(2)	0.0094(8)
	Si	1	3.16(4)	0.0094(8)
	Si	1	3.42(2)	0.0094(8)
2	O	2	1.89(3)	0.008(4)
		2	2.00(3)	0.008(4)
	Si	1	2.74(2)	0.009(2)
	Si	1.9(7)	3.13(2)	0.009(2)
3	O	4	1.94(1)	0.014(1)
	Si	1.6(7)	3.12(2)	0.009(4)
4	O	4	1.97(7)	0.0099(6)
	Si	2.0(8)	3.15(2)	0.011(4)

[a]Average bond lengths from X-ray crystal structure for comparison. [b]Co−X paths measured by EXAFS simulation.
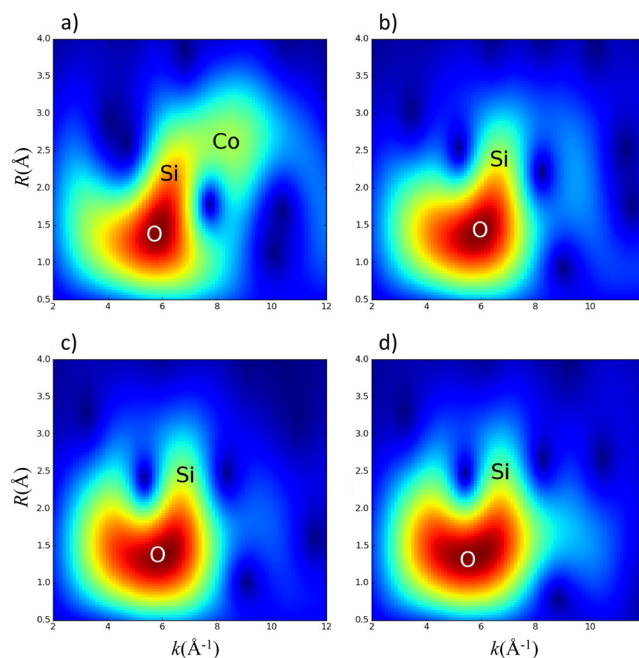
Figure 3. Wavelet transform (WT) analysis of EXAFS data from materials **1** (a), **2** (b), **3** (c), and **4** (d).

Thus, EXAFS, UV−vis, and grafting stoichiometry data all suggest that the surface sites are monomeric, four coordinate, pseudotetrahedral Co(II) with empty coordination sites.

Reactivity of Surface Species (3/4). *Dehydrogenation of Alkanes Catalyzed by 3*. We tested the reactivity of the well-defined surface species **3** toward propane dehydrogenation at 550 °C. Species **3** catalytically converts propane (20% in Ar, 70 mol of propane (mol of Co)$^{-1}$ h^{-1}) into propene with an initial

activity of 12.6 mol of C_3H_8 (mol of Co)$^{-1}$ h^{-1} (3.5×10^{-3} mol of C_3H_8 (mol of Co)$^{-1}$ s^{-1}) that steadily decreased until reaching a plateau at 5 mol of C_3H_8 (mol of Co)$^{-1}$ h^{-1} (10 h) (conversions between 5% and 10%, see Figure 4). Propene production is
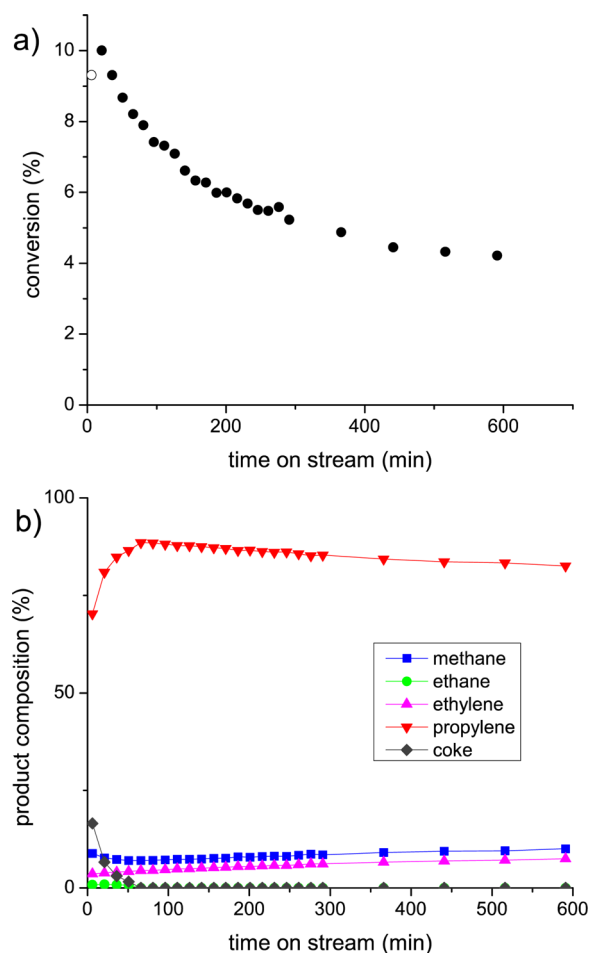
Figure 4. Evolution of (a) conversion and (b) selectivities as a function of time on stream in the propane dehydrogenation catalyzed by **3** (the first data point shown as an empty circle was taken before the stream was fully equilibrated).

accompanied by the formation of ethylene and methane in ca. 1:1 ratio. In addition, the excess of H$_2$ indicates coke formation. Indeed, coke production is a common side reaction in propane dehydrogenation, converting propane into C$_{(s)}$ and 4 equiv of H$_2$. In order to quantify how much carbon was produced, we quantified the amount of H$_2$ produced during the course of the reaction. The amount of coke can be calculated based on the excess of produced H$_2$. The selectivity at the beginning of the reaction was 8:1:2 C_3H_6/C_2H_4/coke. However, coke formation quickly drops off within the first few hours on stream until the rate of coke formation was negligible. This drop in coke formation was accompanied by an increase in selectivity toward propene and ethylene, that reaches 12.3:1 C_3H_6/C_2H_4 after 1.5 h on stream. After this time, the selectivity decreased somewhat until reaching a plateau at 10 h of 8.3:1 C_3H_6/C_2H_4.

The activity above is about an order of magnitude higher than that reported for isolated Co(II) prepared via impregnation (12−5 h^{-1} vs 0.7−1.8 h^{-1}), possibly indicating the presence of more active sites and pointing out the advantage of the thermolytic precursor approach toward the formation of better-defined

supported catalysts.[4b] During the course of the dehydrogenation test, the appearance of the catalyst changed from light blue to black after the reaction, consistent with coke formation. Analysis of the catalyst after reaction confirmed that coke had formed on the surface (11.87 wt % C). We also observed a shift of the edge energy in the XANES spectrum along with disappearance of the pre-edge feature (Figure S15). Comparison of the XANES spectrum of the spent catalyst with that of Co-foil suggests that Co particles are probably forming during catalysis. TEM analysis showed that particles had indeed formed during catalysis with a very wide distribution of 5 ± 2 nm and some particles up to 45 nm in diameter (Figure S16). Carbon nanofibrils had grown off of many of these Co particles, similar to what has been seen with Ni particles.[21]

Catalyst **3** also dehydrogenated isobutane under identical conditions giving a mixture of isobutene, propene, propane, ethene, and methane (conversions between 6−10%, selectivity shown in Figure S17). The TOF of this reaction was initially 18 mol of C_4H_{10} (mol of Co)$^{-1}$ h^{-1} and decayed to a TOF of 11 mol of C_4H_{10} (mol of Co)$^{-1}$ h^{-1} after 10 h on stream (Figure S17). The catalyst also appeared black after the reaction suggesting that particle and coke formation also occurred.

Hydrogenation of Propene Catalyzed by 3. Not surprisingly, **3** also catalyzed the reverse reaction, the hydrogenation of propene. At 50 °C, under a flow of 18 mol of propene (mol of Co)$^{-1}$ h^{-1} and 90 mol of hydrogen (mol of Co)$^{-1}$ h^{-1}, catalyst **3** hydrogenated propene with a TOF = 0.94 h^{-1}, which was the same after 36 h on stream, and the kinetic study discussed below showed good stability of the catalysts under these conditions. We investigated this reaction by varying the temperature (between 50 and 250 °C) and the flow rates (between 18 and 370 mol propene (mol of Co)$^{-1}$ h^{-1} and 90 and 530 mol hydrogen (mol of Co)$^{-1}$ h^{-1}). The rate of the reaction was first order in H$_2$ pressure and showed saturation behavior in propene pressure (K_B = 7(3) bar^{-1}, Figure S18). Eyring analysis of the reaction gave activation parameters of $\Delta H^{\ddagger}$ = 11 kcal mol^{-1} and $\Delta S^{\ddagger}$ = −39 cal mol^{-1} K^{-1}. We also measured the isotope effect upon replacing H$_2$ with D$_2$ at a variety of temperatures and propene pressures (Figure S18). We observed a normal isotope effect of 1.3(2) at 50 °C that increased with increasing temperature until reaching a peak of 2.7(2) at 125 °C. The isotope effect decreased at higher temperatures until reaching 0.9(2) at 225 °C. The isotope effects did not change upon changing the pressure of propylene.

We also used extra-kinetic experiments to probe the mechanism of this reaction further. When propene is reacted with D$_2$ in the presence of **3**, at low conversion only 1,2-dideuteropropane is formed with no D scrambling into propene (Figure S24). The mechanism was further probed by the parahydrogen-induced polarization (PHIP) technique.[22] To this end, heterogeneous hydrogenation of propene was carried out using **3** as catalyst with either normal H$_2$ or parahydrogen-enriched H$_2$ (the ratio of ortho and para isomers o/p = 3:1 and 1:1, respectively). Catalyst **3** was found to be active in propene hydrogenation under the conditions of the experiment (see ESI). The in situ ^{1}H NMR spectrum (Figure 5, bottom) shows only a very weak signal at the chemical shift of propane (as shown by *) under normal hydrogen. The low conversion observed is the result of the experimental conditions not being optimal for high conversions (high flow rates) with the equipment and protocols used in the PHIP studies. However, with parahydrogen, a clear antiphase pattern is observed for the two signals associated with the methylene and methyl groups of propane (top spectrum in Figure 5).

Figure 5. ^{1}H NMR spectra recorded *in situ* during heterogeneous hydrogenation of propene to propane with parahydrogen (top) and normal hydrogen (bottom) catalyzed by **3** (potential propane signal marked with *).

The fact that polarization levels observed are not high could be the result of the paramagnetic nature of the catalyst, which is expected to lead to a significant relaxation of polarization in the reaction intermediates as well as the product (propane) before it can be detected. In addition, low conversion of propene also limits the amount of polarized propane produced in the reaction. Nevertheless, observation of the polarized antiphase signals of propane serves as a clear indication that the pairwise hydrogen addition route is involved in the reaction mechanism.[23] However, the expected significant paramagnetic losses of polarization mentioned above make it impossible to estimate the contribution of this pairwise route to the overall reaction mechanism at present.

In order to investigate the activation of H_2 alone, we attempted to observe the reaction of H_2 with the catalyst. The catalyst did not appear to react with H_2 under conditions of normal pressure. However, in the presence of **3** at 50 °C in toluene, we found that 40 atm of D_2 exchanged with $HOSi(OtBu)_3$ (**5**) to produce 13% $DOSi(OtBu)_3$ (**5**-d_1), which we observed by both ^{1}H and ^{2}H NMR (Figure S25).

Reaction of Terminal Alkynes with 3/4. We also investigated the reactivity of **3** toward propyne and other alkynes. At 25 °C, **3** catalyzes the trimerization of terminal alkynes, for example, propyne and 3,3-dimethylbutyne. Investigation of the reaction of **3** with 450 mbar of $tBuC\equiv CH$ by IR spectroscopy shows that new IR bands appear in the C−H stretching and bending regions along with new C≡C stretches at 2133 and 2100 cm^{-1} (Figure S22), accompanied by a vibrant color change from light blue to purple. These peaks do not appear in the absence of Co on the surface indicating that these bands are due to alkyne bound to the Co sites. Upon heating, disappearance of the bands at 2133 and 2100 cm^{-1} is accompanied by the appearance of new bands at 3070, 3040, 1681, and 1595 cm^{-1}. These bands can be assigned as aromatic C−H stretches (3070 and 3040 cm^{-1}) and aromatic C=C stretches (1681 and 1595 cm^{-1}) of the newly formed trimers.[24] Surface Co species **3** and **4** also trimerize propyne with a 1:2 selectivity of 1,3,5:1,2,4 product (See ^{1}H NMR

and GC/MS in Figure S20). However, these catalysts do not react with internal alkynes like 2-butyne.

$$\frac{d[\mathbf{5}]}{dt} = \frac{k_{obs}n_{Co}[1\text{-octyne}]}{[\mathbf{5}\text{-}d_1]} \tag{2}$$

$$\frac{d[\mathbf{5}]}{dt} = k_{oobsbs}[\mathbf{1}][1\text{-octyne}]\frac{K_{eq}}{K_{eq} + [\mathbf{5}\text{-}d_1]} \tag{3}$$

Addition of an excess of $HOSi(OtBu)_3$ (**5**) to the reaction of 1-octyne and **3** inhibits the trimerization. Furthermore, when the experiment is carried out with an excess of $DOSi(OtBu)_3$ (**5**-d_1), D-incorporation into the sp C−H bond of 1-octyne occurs (eq 1), suggesting that C−H bond activation occurs during this process. However, we also observed H/D exchange between $tBuCCD$ and SiO_{2-700} alone (Figure S23). Thus, H/D exchange catalyzed by **3** could occur through the surface hydroxyls instead of through the Co sites. In order to obtain evidence for or against acid-catalyzed exchange, we replaced catalyst **3** with **4**, in which all exchangeable protons have been replaced with $SiMe_3$ groups. Under the same reaction conditions, **4** also catalyzed the H/D exchange between 1-octyne and **5**-d_1. Next, we measured the rate law of 1-octyne H/D exchange (eq 1) catalyzed by **4**. We performed kinetic experiments at 40 °C with 1-octyne as the limiting reagent and **5**-d_1 in excess. Excess **5**-d_1 pushed the equilibrium of eq 1 to the right (>95% yield) and ensured that the back reaction did not interfere with our rate measurements. We were able to follow the reaction by monitoring the appearance of the SiOH peak in the ^{1}H NMR (see SI for full details of the kinetic experiments). In order to avoid diffusion problems within the NMR tube, we agitated the solution while submerged in a constant temperature bath at 40 °C and periodically sampled the reaction over the course of 8−12 hours. We found that the rate law was first order in 1-octyne, first order in the cobalt loading on **4**, and inverse order in **5**-d_1 (Figure S27, eq 2). The rate constant k_{obs} is 6.8×10^{-3} M mmol^{-1} s^{-1} at 40 °C.

$$Co_2(OSi(OtBu)_3)_4(DOSi(OtBu)_3) \underset{}{\overset{K_{dissoc}}{\rightleftharpoons}} Co_2(OSi(OtBu)_3)_4 + DOSi(OtBu)_3 \tag{4}$$
$$\mathbf{1} \qquad \mathbf{5}\text{-}d_1$$

$$H\equiv\!\!=\!\!-R + Co_2(OSi(OtBu)_3)_4 \underset{k_{-H}\,(fast)}{\overset{k_H}{\rightleftharpoons}} Co_2(OSi(OtBu)_3)_3(CCR) + HOSi(OHtBu)_3 \tag{5}$$
$$\mathbf{1} \qquad \mathbf{6} \qquad \mathbf{5}$$

$$\left[\begin{array}{c} Si(OtBu)_3 \\ Co\!-\!O \\ \equiv\!\!\cdots H \\ R \end{array}\right]^{\ddagger}$$

$$Co_2(OSi(OtBu)_3)_3(CCR) + DOSi(OtBu)_3 \underset{k_D}{\overset{k_{-D}\,(fast)}{\rightleftharpoons}} D\equiv\!\!=\!\!-R + Co_2(OSi(OtBu)_3)_4 \tag{6}$$
$$\mathbf{6} \qquad \mathbf{5}\text{-}d_1 \qquad \mathbf{1}$$

$$\frac{d[\mathbf{5}]}{dt} = \frac{k_H k_{-D}[Co][1\text{-octyne}][\mathbf{5}\text{-}d_1]}{k_{-H}[\mathbf{5}] + k_{-D}[\mathbf{5}\text{-}d_1]} - \frac{k_D k_{-H}[Co][1\text{-octyne-}d_1][\mathbf{5}]}{k_{-H}[\mathbf{5}] + k_{-D}[\mathbf{5}\text{-}d_1]} \tag{7}$$

where $\quad [Co] = \dfrac{[\mathbf{1}]_{total}K_{eq}}{K_{eq} + [\mathbf{5}\text{-}d_1]} \tag{8}$

if $\quad [\mathbf{5}\text{-}d_1] \gg [\mathbf{5}] \tag{9}$

then $\quad \dfrac{d[\mathbf{5}]}{dt} = k_H[Co][1\text{-octyne}]$

$$- k_D\frac{k_{-H}}{k_{-D}}[Co][1\text{-octyne-}d_1]\frac{[\mathbf{5}]}{[\mathbf{5}\text{-}d_1]}$$

$$\approx k_H[Co][1\text{-octyne}] \tag{10}$$

Hex$\equiv$H
$\quad +$
$DOSi(OtBu)_3$
5-d_1

$\underset{}{\overset{1\ or\ 4\ (cat)}{\rightleftharpoons}}$

Hex$\equiv$D
$\quad +$
$HOSi(OHtBu)_3$
5

(1)

C−H Activation by Molecular Analog Co₂(OSi(OtBu)₃)₄ (1). We then investigated the reactivity of **1** in the H/D exchange between terminal alkynes and silanols, analogous to the corresponding surface species **3** and **4**. The thermal stability of **1** does not allow investigation of its reactivity toward alkenes or alkanes at high temperatures (**1** decomposes slowly above 55 °C). As shown for the supported complexes, the molecular analog **1** reacts with propyne to give a 1:1.9 mixture of 1,3,5:1,2,4 trimethylbenzene regioisomers (¹H NMR and GC/MS shown in SI Figure S19). Like the surface species **4**, **1** does not react with internal alkynes. In the presence of excess **5**, no alkyne trimerization occurs. The addition of excess DOSi(OtBu)₃ (**5**-d_1) causes D scrambling into the terminal alkyne position (¹H and ²H NMR Figure S21). In order to further interrogate the mechanism, we determined the rate law of this H/D exchange. The rate law is first order in [1-octyne], first order in [**1**], and weakly inhibited by [**5**-d_1] (Figure S26, eq 3). The experimental rate law is shown in eq 3. We obtained values of $k_H = 1.26(6) \times 10^{-2} \ M^{-1} \ s^{-1}$ and $K_{eq} = 0.6(2) \ M$, where K_{eq} is the pre-equilibrium dissociation constant of **5**-d_1 from cobalt (eq 4).

We measured the H/D deuterium isotope effect by monitoring the rate of exchange of 1-octyne-d_1 with **5** (reverse of eq 1). Because of overlapping resonances in the ¹H NMR spectrum, we were not able to monitor this reaction by NMR. Instead we measured the disappearance of 1-octyne-d_1 by IR spectroscopy in a ReactIR system (Figures S31 and S32). We also repeated the reaction of 1-octyne with **5**-d_1 under identical conditions for direct comparison. These experiments yielded a kinetic isotope effect $k_H/k_D = 1.7(4)$.

■ DISCUSSION

Kinetics and Mechanism of H/D Exchange Reaction. The rate laws for both homogeneous (**1**) and heterogeneous (**4**) H/D exchange reactions have a few characteristics in common: (1) They are both first order in Co and 1-octyne. (2) Both are inhibited by excess silanol in the solution (although in the case of **1** this inhibition could almost be considered zero-order, Figure S25). Pre-equilibrium dissociation of silanol from the active site is a natural consequence of the Lewis acidity of the active sites and would be present no matter what rate-determining step followed. This is consistent with a rate-determining step involving only 1-octyne and **1** or **4**. In addition, the nuclearity of the complex does not seem to play a role, since both the monomeric **4** and dimeric **1** are catalysts.

We hypothesize that C−H activation occurs through a mechanism like that shown in eqs 4−6. This mechanism involves C−H activation on the Co active site as the rate-determining step (eq 4 and 5). The bond-breaking step would involve the four-membered transition state shown in eq 6 (characteristic of 1,2-addition) in which the lone pair on the siloxide would play an important role.[5e] The C−H activation step is presumably followed by rapid reaction with **5**-d_1 to produce 1-octyne-d_1 (eq 6). The full rate law for this mechanism is shown in eqs 7 and 8. In the limit of high [**5**-d_1], this full rate law simplifies to a rate law that is equal to the one we determined experimentally (eq 10). This mechanism is consistent with previous studies on molecular complexes: HRu(OSiPh₃)(PtBu₃)₂(CO) reacts with PhCCH through C−H activation on Ru-OSiPh₃ to produce HRu(CCPh)(PtBu₃)₂(CO) and HOSiPh₃,[25] and similar mechanisms have been proposed for benzene C−H activation by Ir−OR,[5c,d] Ru−OR,[26] and Pd−OR complexes[27] as well as for activation of indene by Rh−OH complexes[28]

However, alternative mechanisms have been proposed, involving metallacycle intermediates or stepwise processes. For instance, in the C−H activation of a variety of C−H bonds to imido Zr species **7**,[29] the rate of addition of *t*-butylacetylene to **7** was much faster than any other C−H bond and involved an inverse H/D kinetic isotope effect (KIE) of 0.8, while the others possessed large KIEs of 5−8. These data were consistent with the overall 1,2-addition of *t*-butylacetylene through a metallacycle intermediate **8** (eq 11) rather than a simple four-membered

$$Cp^*CpZr=NtBu \xrightarrow{\quad} Cp^*CpZr-NtBu \xrightarrow{\quad} Cp^*CpZr-NHtBu \qquad (11)$$
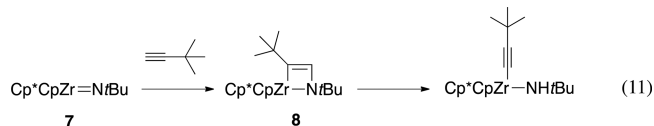
transition state. The KIE observed with the Co catalyst studied here of 1.7(4) is consistent with C−H bond breaking being at or before the rate-determining step of the reaction. This value, however, is significantly smaller than the KIE's found for some other 1,2-addition reactions such as the C−H bond activation on early transition metal imido complexes, which often display large KIEs between 5 and 7.[30] However, it has also been reported that the 1,2-addition of benzene on (py)(acac)₂IrOH displays a KIE of 2.6(5), close to our value of 1.7(4).[5d] Thus, the data collected above for the H/D exchange between **5**-d_1 and 1-octyne catalyzed by **1** or **4** is consistent with this mechanism.

C−H activation of terminal alkynes can also occur in a stepwise fashion.[31] For instance, coordinatively saturated late transition metal amido complexes can react by first deprotonating the terminal alkyne to form an ion pair between the cationic metal fragment and the alkyl acetylide anion, which then reacts further to form the metal acetylide bond. While possible, this mechanism is less likely for the Co-system studied here because (i) siloxide ligands are much less basic than the ligands used in the literature examples (amides and alkoxides), (ii) Co is coordinatively unsaturated in contrast to the other systems discussed above, and (iii) the reaction medium is very nonpolar, discouraging ion-pair formation.

Late transition-metal alkoxide complexes are known to dissociate in nonpolar solutions to a small extent in some cases.[32] One could envision that, rather than a direct 1,2-addition, the ion pair [Co]⁺[OSi(OtBu)₃]⁻ could potentially deprotonate coordinated alkynes without going through a 1,2-addition type transition state. Based on the data, we cannot rule out this mechanism. However, this reaction usually occurs for coordinatively saturated species, in which the dissociation of the ligand is necessary for the reaction to occur. Since our complexes are coordinatively unsaturated, the dissociation of the ligand is not necessary for the reaction to occur.

One interesting difference between the homogeneous and heterogeneous rate law is the change in silanol dependence. In the homogeneous H/D exchange, silanol concentration only weakly inhibits the reaction, whereas in the heterogeneous H/D exchange, the rate law is true inverse order in **5**-d_1. If we once again consider the simplified rate law in eq 10, in the limit of [**5**-d_1] being much larger than K_{eq}, the rate law further simplifies to eq 13. Here, the observed rate constant for the reaction is the product of the dissociation constant (K_{eq}) and the rate constant for C−H activation (k_H). Since the homogeneous and heterogeneous experiments were performed at similar [**5**-d_1] (between 0.1 and 1.5 M), this must mean that **5**-d_1 binds more strongly (smaller K_{eq}) to **4** than to **1**.
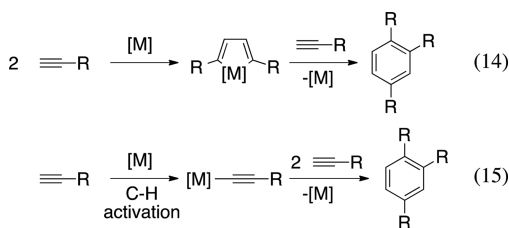
In the case of the heterogeneous reaction where **4** is the catalyst, we cannot measure the precise value of K_{eq}. However, we can estimate an upper limit. In order to observe the rate law in eq 13, inequality 12 must be satisfied. This means that the smallest $[\mathbf{5}\text{-}d_1]$ that we used is at least an order of magnitude greater than $K_{eq,4}$. Thus, $K_{eq,4}$ must be ≤ 0.0125 M.

$$\text{if} \qquad [\mathbf{5}\text{-}d_1] \gg K_{eq} \tag{12}$$

$$\text{then} \qquad \frac{d[\mathbf{5}]}{dt} = k_H[1\text{-octyne}] \frac{n_{Co} K_{eq}}{K_{eq} + [\mathbf{5}\text{-}d_1]}$$

$$\approx \frac{k_H K_{eq} n_{Co}[1\text{-octyne}]}{[\mathbf{5}\text{-}d_1]} \tag{13}$$

In other words, $K_{eq,1}$ is at least 48 times larger than $K_{eq,4}$ or **5** binds more strongly to **4** than to **1**. This difference in binding may be caused by greater Lewis acidity of **4** than **1** or by greater van der Waals interactions of **5** with the surface.[33] Thus, while we can say that species **4** binds ligands more strongly than **1**, we cannot say that this is directly caused by increased Lewis acidity of the metal center. However, increased Lewis acidity could be the reason that CO binds to **3** but not **1** or **2**.

Mechanism of Alkyne Trimerizations by 1, 3, and 4. We found that **1**, **3**, and **4** catalyze alkyne trimerization in the absence of **5**. Both homogeneous and heterogeneous catalysts have the same regioselectivity for the reaction suggesting that they operate with similar mechanisms. Alkyne trimerization is thought to occur by a variety of different mechanisms, such as [2 + 2 + 2]-cycloaddition (eq 14, often catalyzed by low-valent Co species)[34] or, alternatively, via C−H activation followed by insertion (eq 15).[35] The latter mechanism often gives both dimeric (eneyne) and trimeric products.[36] In our case, the fact that our catalysts do not trimerize internal alkynes makes the former mechanism (eq 14) unlikely. Mechanisms involving oxidative coupling, such as eq 14, will probably also be disfavored since

$$2 \ \equiv\!\!-R \xrightarrow{[M]} R \overset{[M]}{\diagdown} R \xrightarrow[\text{-[M]}]{\equiv\!\!-R} \text{(arene)} \tag{14}$$

$$\equiv\!\!-R \xrightarrow[\text{C-H activation}]{[M]} [M]\!\!\equiv\!\!-R \xrightarrow[\text{-[M]}]{2 \ \equiv\!\!-R} \text{(arene)} \tag{15}$$

they would lead to the formation of Co(IV) centers. Also, the fact that addition of **5** suppresses trimerization along with the observation of H/D exchange in the presence of **5**-d_1 are both consistent with a mechanism involving C−H activation (Scheme 1). In this mechanism, addition of **5** to the reaction lowers the concentration of intermediate **6**, inhibiting the trimerization.

Mechanistic Conclusions on Propene Hydrogenation. We showed above that **3** and **4** can react with alkynes by C−H activation. We have shown that these catalysts also hydrogenate propene above 50 °C and that the rate law of this reaction is first order in $P(H_2)$ and saturates in $P(C_3H_6)$. We observe polarization of ^1H NMR signals of propane in the PHIP experiment and only 1,2-dideuteropropane in the reaction of D_2 with propene catalyzed by **3**. These results are consistent with the addition of both hydrogen atoms from the same H_2 molecule to propene.[22b] The absence of deuterium incorporation into propene when using D_2 confirms that the insertion step is irreversible under the explored reaction conditions. We also observed that the

**Scheme 1. Mechanism of Alkyne Trimerization by 1 Involving C−H Activation**
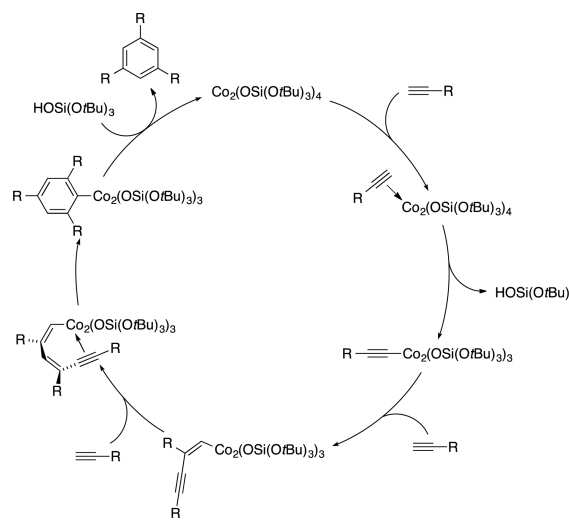
isotope effect is temperature dependent and reaches a maximum of 2.7(1) at 125 °C. This is consistent with the H_2 activation occurring on or before the rate-determining step.

First, the first order dependence on hydrogen pressure implies that the coverage of H_2 on the surface is small. This is consistent with the observation that when only H_2 is added to **3**, we cannot observe any intermediates, showing that the concentration of surface sites with bound H_2 is low. This is also consistent with calculations on a related Cr(III) system on silica that show that activation of the H−H bond is endoenergetic by 37 kcal mol^{-1}.[12c] We have observed that **3** reversibly adsorbs propene, consistent with the binding constant of $K_B = 7(3)$ bar^{-1} that we observed here. Second, the activation parameters ($\Delta H^{\ddagger} = 11$ kcal mol^{-1} and $\Delta S^{\ddagger} = -39$ cal mol^{-1} K^{-1}) show that the transition state is highly ordered in comparison to the reactants. This result, coupled with the observation of polarization transfer during the PHIP experiment, suggests that the reactant molecules must all be adsorbed on the same active site before undergoing reaction. Our observation that D_2 exchanges with **5** in the presence of **3** shows the intermediacy of a metal hydride in the reaction of **3** with H_2/D_2.

If the H−H bond breaking step were the rate-determining step, we might expect a large primary isotope effect. However, what we see is that at lower temperatures, the isotope effect is small $(1.2(1) - 1.6(2))$ then reaches a maximum of 2.7(1) before going back down to 0.9(1). While insertion is probably irreversible, it does not imply that it is the rate-determining step. We also do not know whether the steps before insertion are reversible. Thus, the temperature dependence of the isotope effect could be due to a complex interplay of isotope effects from H_2 coordination ($K_{\sigma\text{-}H_2}$), H_2 splitting (K_{H_2}), and olefin insertion (Scheme 3) and could be explained by a variety of interpretations. One scenario is that insertion is rate determining (due to the low concentration of sites with both propene and H_2 coordinated) and everything before that is reversible (rate law in eq 16). Another possibility is that H_2 splitting is rate-determining and propene coordination occurs before H_2 splitting (rate law in eq 17). In this scenario, the small isotope effects at low temperature would probably be caused by the pre-equilibrium formation of the σ-H_2 complex. This pre-equilibrium is expected to have a temperature dependent isotope effect that is negative at

Scheme 2. Possible Mechanisms for Propene Hydrogenation Catalyzed by 3
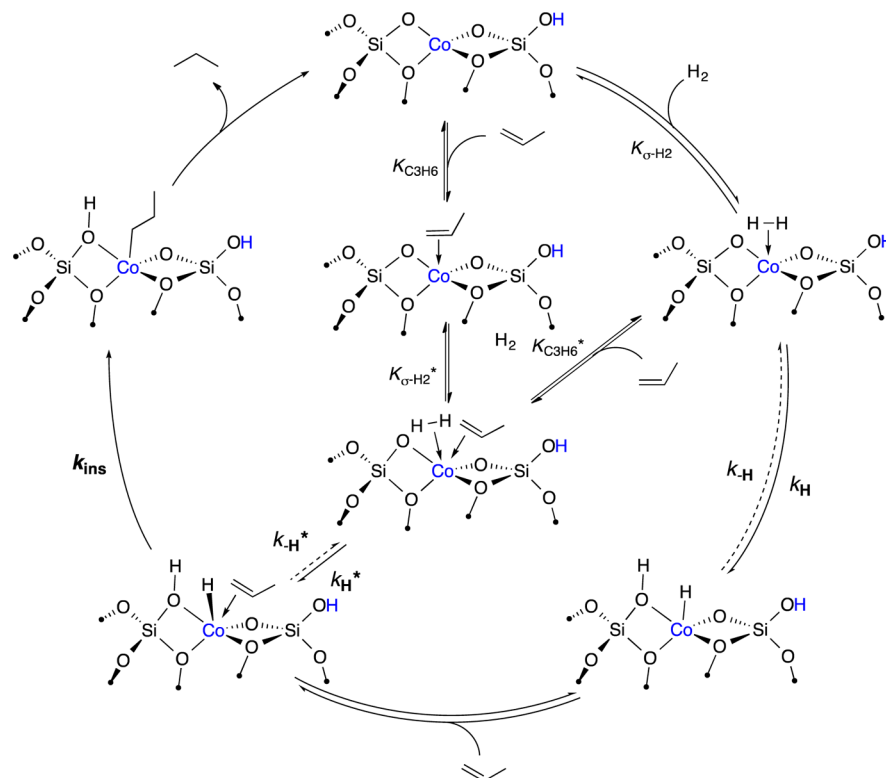
lower temperatures, consistent with the observed temperature dependence.

$$\frac{dn_{C_3H_8}}{dt} = K_{\sigma\text{-}H_2} K_{H_2} k_{ins} P_{H_2} n_{Co} \frac{K_B P_{C_3H_6}}{K_B + P_{C_3H_6}} \tag{16}$$

$$\frac{dn_{C_3H_8}}{dt} = K_{\sigma\text{-}H_2} k_{H_2} P_{H_2} n_{Co} \frac{K_B P_{C_3H_6}}{K_B + P_{C_3H_6}} \tag{17}$$

From these kinetic experiments, the mechanism must take place on a single metal site and involve either oxidative addition or 1,2-addition. However, oxidative addition is unlikely. Indeed, very few examples of oxidative additions to high-spin Co(II) complexes are known.[37] They typically only occur with very electron donating ligands and very good oxidants (such as I_2 or azides). Oxidative addition of reagents like H_2 to an electron-poor high-spin Co(II) such as **3** (making formally Co(IV)-bis hydride) is unlikely.[38] In fact, neither **1** nor **3** reacts with I_2 even at 50 °C (the temperature at which catalysis takes place), showing that oxidative addition on such sites is not likely. On the other hand, 1,2-addition of H_2 across late metal oxygen bonds is ubiquitous. Homogeneous alkoxo and hydroxo complexes of Rh,[39] Pd,[32d,40] Ir,[41] and Cu[42] activate H_2 by 1,2-addition. Lewis acid sites of non-redox-active metals including Al also catalyze H−H activations,[43] suggesting that redox activity of the metal is not required.

Mechanism of Alkane Dehydrogenation by 3. The principle of microscopic reversibility suggests that dehydrogenation and hydrogenation go by similar mechanisms (Scheme 2). This is consistent with DFT calculations by Hock on Co(II) sites[4b] and by our group on Cr(III) sites.[12c] However, other mechanisms must be considered. Transition metal complexes can sometimes abstract H• from alkanes to make alkyl radicals by a proton coupled electron transfer (PCET) or hydrogen atom

transfer (HAT) mechanism.[44] In order to test for such a mechanism, we compared the reactivity of propane and isobutane under the same conditions. If propane and isobutane reacted by a PCET mechanism, then, based on predicted rates of H• transfer, we would expect them to have the same TOF.[45] However, isobutane reacts about 1.6 times faster than propane, proportional to their ratio of primary C−H bonds. In fact, when normalized to the number of primary C−H bonds in each molecule, the initial TOF's of both propane and isobutane are equal (Figure S17). This suggests that **3** may react via primary C−H bonds, consistent with heterolytic splitting rather than homolytic splitting. The selectivity of this catalyst is fairly high. However, the high temperature of this reaction causes many side reactions to interfere with the formation of propene. First, formation of Co particles and coke occur during catalysis. Either (or both) of them could be involved in the deactivation. Besides dehydrogenation, **3** also catalyzes cracking of propane into ethylene and methane, which could occur by several possible mechanisms. At 550 °C, propyl radical decomposes rapidly ($k \approx 10^9 - 10^{10}$ s^{-1}) to form either propene and H• or ethylene and $CH_3^\bullet$ with a 5:1 preference for cracking.[46] This would form a Co(I) center and propyl radical (Scheme 3). It could be that Co−C bond cleavage is a major contributor to the cracking side reaction. However, the preference of propyl radicals for cracking also suggests that PCET/HAT reactions are not occurring to any appreciable extent, since this would result in much lower propene selectivity. Another possibility is that cracking is the result of β-Me transfer,[47] a process that is reasonable at these temperatures. Brønsted acid sites on the support are also known to catalyze cracking.[48]

■ **CONCLUSION**

We have shown that grafting of **1** on SiO_{2-700} yields four-coordinate monomeric surface Co(II) sites. We also showed that this structure is conserved upon subsequent thermal treatment

Scheme 3. Proposed Mechanism of Propane Dehydrogenation Catalyzed by 3
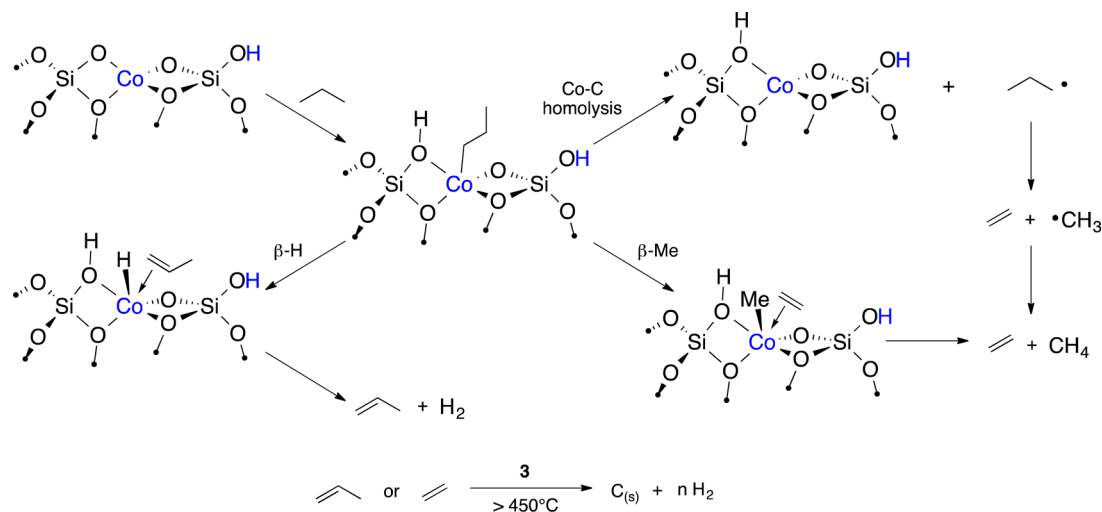
and passivation. We have observed that these Co(II) ions isolated on silica can activate R−H bonds of hydrocarbons, in the dehydrogenation of propane, hydrogenation of propene, and the trimerization of alkynes in aromatics. On the basis of mechanistic investigations on both molecular and supported species, we have shown that C−H and H−H bond activation probably takes place via a 1,2-addition mechanism (heterolytic splitting) on isolated Co(II)−O bonds. This mechanism is similar to what we have recently shown for C−H and H−H activation on Al,O sites[43] and what was proposed for the C−H bond activation of hydrocarbons on Cr(III),O sites.[12c] This C−H activation step may be general to alkane dehydrogenation, alkyne trimerization, and hydrogenation on Co(II),O sites.

ASSOCIATED CONTENT

Ⓢ Supporting Information

The Supporting Information is available free of charge on the ACS Publications website at DOI: 10.1021/jacs.6b08705.

Crystallographic information file of compound 1 (CIF)
Supporting NMR data (ZIP)
General experimental details, synthetic details, material characterization, reaction details, and kinetic measurements (PDF)

AUTHOR INFORMATION

Corresponding Author

*ccoperet@inorg.chem.ethz.ch

Author Contributions

All authors have given approval to the final version of the manuscript.

Notes

The authors declare no competing financial interest.

ACKNOWLEDGMENTS

REFERENCES

(1) (a) Copéret, C. *Chem. Rev.* **2010**, *110*, 656. (b) Latimer, A. A.; Kulkarni, A. R.; Aljama, H.; Montoya, J. H.; Yoo, J. S.; Tsai, C.; Abild-Pedersen, F.; Studt, F.; Norskov, J. K. *Nat. Mater.* **2016**, DOI: 10.1038/nmat4760. (c) Santoro, S.; Kozhushkov, S. I.; Ackermann, L.; Vaccaro, L. *Green Chem.* **2016**, *18*, 3471.

(2) (a) Weckhuysen, B. M.; Wachs, I. E.; Schoonheydt, R. A. *Chem. Rev.* **1996**, *96*, 3327. (b) Carrero, C. A.; Schloegl, R.; Wachs, I. E.; Schomaecker, R. *ACS Catal.* **2014**, *4*, 3357. (c) Sattler, J. J. H. B.; Gonzalez-Jimenez, I. D.; Luo, L.; Stears, B. A.; Malek, A.; Barton, D. G.; Kilos, B. A.; Kaminsky, M. P.; Verhoeven, T. W. G. M.; Koers, E. J.; Baldus, M.; Weckhuysen, B. M. *Angew. Chem., Int. Ed.* **2014**, *53*, 9251. (d) Sattler, J. J. H. B.; Ruiz-Martinez, J.; Santillan-Jimenez, E.; Weckhuysen, B. M. *Chem. Rev.* **2014**, *114*, 10613.

(3) (a) Baudry, D.; Ephritikhine, M.; Felkin, H. *J. Chem. Soc., Chem. Commun.* **1982**, 606. (b) Baudry, D.; Ephritikhine, M.; Felkin, H.; Holmes-Smith, R. *J. Chem. Soc, Chem. Commun.* **1983**, 788. (c) Haenel, M. W.; Oevers, S.; Angermund, K.; Kaska, W. C.; Fan, H.-J.; Hall, M. B. *Angew. Chem., Int. Ed.* **2001**, *40*, 3596. (d) Dobereiner, G. E.; Crabtree, R. H. *Chem. Rev.* **2010**, *110*, 681 and references therein. (e) Choi, J.; MacArthur, A. H. R.; Brookhart, M.; Goldman, A. S. *Chem. Rev.* **2011**, *111*, 1761.

(4) (a) Schweitzer, N. M.; Hu, B.; Das, U.; Kim, H.; Greeley, J.; Curtiss, L. A.; Stair, P. C.; Miller, J. T.; Hock, A. S. *ACS Catal.* **2014**, *4*, 1091. (b) Hu, B.; "Bean" Getsoian, A.; Schweitzer, N. M.; Das, U.; Kim, H.; Niklas, J.; Poluektov, O.; Curtiss, L. A.; Stair, P. C.; Miller, J. T.; Hock, A. S. *J. Catal.* **2015**, *322*, 24. (c) Hu, B.; Schweitzer, N. M.; Zhang, G.; Kraft, S. J.; Childers, D. J.; Lanci, M. P.; Miller, J. T.; Hock, A. S. *ACS Catal.* **2015**, *5*, 3494.

(5) (a) Walsh, P. J.; Hollander, F. J.; Bergman, R. G. *J. Am. Chem. Soc.* **1988**, *110*, 8729. (b) Bennett, J. L.; Wolczanski, P. T. *J. Am. Chem. Soc.* **1997**, *119*, 10696. (c) Tenn, W. J.; Young, K. J. H.; Bhalla, G.; Oxgaard, J.; Goddard, W. A.; Periana, R. A. *J. Am. Chem. Soc.* **2005**, *127*, 14172. (d) Tenn, W. J.; Young, K. J. H.; Oxgaard, J.; Nielsen, R. J.; Goddard, W. A.; Periana, R. A. *Organometallics* **2006**, *25*, 5173. (e) Webb, J. R.; Burgess, S. A.; Cundari, T. R.; Gunnoe, T. B. *Dalton Trans.* **2013**, *42*, 16646.

(6) (a) Espenson, J. H. *Chemical Kinetics and Reaction Mechanisms*, 2nd ed.; Mcgraw Hill Custom Publishing: New York, 1981. (b) Novstrup, K. A.; Travia, N. E.; Medvedev, G. A.; Stanciu, C.; Switzer, J. M.; Thomson, K. T.; Delgass, W. N.; Abu-Omar, M. M.; Caruthers, J. M. *J. Am. Chem. Soc.* **2010**, *132*, 558.

(7) Boudart, M.; Djega-Mariadassou, G. *Kinetics of Heterogeneous Catalytic Reactions*; Princeton University Press: Princeton, NJ, 1984.

(8) (a) Feher, F. J.; Newman, D. A.; Walzer, J. F. *J. Am. Chem. Soc.* **1989**, *111*, 1741. (b) Marciniec, B.; Maciejewski, H. *Coord. Chem. Rev.* **2001**, *223*, 301. (c) Cordes, D. B.; Lickiss, P. D.; Rataboul, F. *Chem. Rev.* **2010**, *110*, 2081. (d) Quadrelli, E. A.; Basset, J.-M. *Coord. Chem. Rev.* **2010**, *254*, 707.

(9) (a) Nozaki, C.; Lugmair, C. G.; Bell, A. T.; Tilley, T. D. *J. Am. Chem. Soc.* **2002**, *124*, 13194. (b) König, S. N.; Maichle-Mössmer, C. c.; Törnroos, K. W.; Anwander, R. *Z. Naturforsch., B: J. Chem. Sci.* **2014**, *69*, 1375.

(10) (a) Marks, T. J. *Acc. Chem. Res.* **1992**, *25*, 57. (b) Copéret, C.; Chabanas, M.; Petroff Saint-Arroman, R.; Basset, J.-M. *Angew. Chem., Int. Ed.* **2003**, *42*, 156. (c) Fierro-Gonzalez, J. C.; Gates, B. C. *Chem. Soc. Rev.* **2008**, *37*, 2127. (d) Wegener, S. L.; Marks, T. J.; Stair, P. C. *Acc. Chem. Res.* **2012**, *45*, 206. (e) Copéret, C.; Comas-Vives, A.; Conley, M. P.; Estes, D. P.; Fedorov, A.; Mougel, V.; Nagae, H.; Núñez-Zarur, F.; Zhizhko, P. A. *Chem. Rev.* **2016**, *116*, 323.

(11) (a) Fujdala, K. L.; Tilley, T. D. *Chem. Mater.* **2001**, *13*, 1817. (b) Brutchey, R. L.; Drake, I. J.; Bell, A. T.; Tilley, T. D. *Chem. Commun.* **2005**, 3736. (c) Fujdala, K.; Brutchey, R.; Tilley, T. D. In *Surface and Interfacial Organometallic Chemistry and Catalysis*; Copéret, C., Chaudret, B., Eds.; Springer: Berlin Heidelberg, 2005; Vol. 16, p 69.

(12) (a) Conley, M. P.; Delley, M. F.; Siddiqi, G.; Lapadula, G.; Norsic, S.; Monteil, V.; Safonova, O. V.; Copéret, C. *Angew. Chem., Int. Ed.* **2014**, *53*, 1872. (b) Delley, M. F.; Núñez-Zarur, F.; Conley, M. P.; Comas-Vives, A.; Siddiqi, G.; Norsic, S.; Monteil, V.; Safonova, O. V.; Copéret, C. *Proc. Natl. Acad. Sci. U. S. A.* **2014**, *111*, 11624. (c) Conley, M. P.; Delley, M. F.; Núñez-Zarur, F.; Comas-Vives, A.; Copéret, C. *Inorg. Chem.* **2015**, *54*, 5065.

(13) Mougel, V.; Chan, K.-W.; Siddiqi, G.; Kawakita, K.; Nagae, H.; Tsurugi, H.; Mashima, K.; Safonova, O.; Copéret, C. *ACS Cent. Sci.* **2016**, *2*, 569.

(14) Rendón, N.; Bourdolle, A.; Baldeck, P. L.; Le Bozec, H.; Andraud, C.; Brasselet, S.; Copéret, C.; Maury, O. *Chem. Mater.* **2011**, *23*, 3228.

(15) Göltl, F.; Hafner, J. *J. Chem. Phys.* **2012**, *136*, 064503.

(16) (a) Ferrari, A. M.; Neyman, K. M.; Rösch, N. *J. Phys. Chem. B* **1997**, *101*, 9292. (b) Lupinetti, A. J.; Strauss, S. H.; Frenking, G. In *Progress in Inorganic Chemistry*; Karlin, K. D., Ed.; John Wiley & Sons, Inc.: New York, 2001; Vol. 49, p 1. (c) Zecchina, A.; Scarano, D.; Bordiga, S.; Spoto, G.; Lamberti, C. In *Advances in Catalysis*; Gates, B. C., Knoezinger, H., Eds.; Academic Press: San Diego, CA, 2001; Vol. 46, p 265.

(17) Sigel, G. A.; Bartlett, R. A.; Decker, D.; Olmstead, M. M.; Power, P. P. *Inorg. Chem.* **1987**, *26*, 1773.

(18) Cotton, F. A.; Goodgame, D. M. L.; Goodgame, M. *J. Am. Chem. Soc.* **1961**, *83*, 4690.

(19) Han, J.; Woo, S. *Korean J. Chem. Eng.* **1991**, *8*, 235.

(20) (a) Funke, H.; Chukalina, M.; Scheinost, A. C. *J. Synchrotron Radiat.* **2007**, *14*, 426. (b) Timoshenko, J.; Kuzmin, A. *Comput. Phys. Commun.* **2009**, *180*, 920. (c) Penfold, T. J.; Tavernelli, I.; Milne, C. J.; Reinhard, M.; Nahhas, A. E.; Abela, R.; Rothlisberger, U.; Chergui, M. *J. Chem. Phys.* **2013**, *138*, 014104.

(21) Huh, Y.; Green, M. L. H.; Kim, Y. H.; Lee, J. Y.; Lee, C. J. *Appl. Surf. Sci.* **2005**, *249*, 145.

(22) (a) Bowers, C. R.; Weitekamp, D. P. *J. Am. Chem. Soc.* **1987**, *109*, 5541. (b) Salnikov, O. G.; Kovtunov, K. V.; Barskiy, D. A.; Bukhtiyarov, V. I.; Kaptein, R.; Koptyug, I. V. *Appl. Magn. Reson.* **2013**, *44*, 279.

(23) (a) Kovtunov, K. V.; Zhivonitko, V. V.; Skovpin, I. V.; Barskiy, D. A.; Koptyug, I. V. In *Hyperpolarization Methods in NMR Spectroscopy*; Kuhn, T. L., Ed.; Springer: Berlin, Heidelberg, 2013; p 123. (b) Ananikov, V. P.; Khemchyan, L. L.; Ivanova, Y. V.; Bukhtiyarov, V. I.; Sorokin, A. M.; Prosvirin, I. P.; Vatsadze, S. Z.; Medved'ko, A. V.; Nuriev, V. N.; Dilman, A. D.; Levin, V. V.; Koptyug, I. V.; Kovtunov, K. V.; Zhivonitko, V. V.; Likholobov, V. A.; Romanenko, A. V.; Simonov, P. A.; Nenajdenko, V. G.; Shmatova, O. I.; Muzalevskiy, V. M.; Nechaev, M. S.; Asachenko, A. F.; Morozov, O. S.; Dzhevakov, P. B.; Osipov, S. N.; Vorobyeva, D. V.; Topchiy, M. A.; Zotova, M. A.; Ponomarenko, S. A.; Borshchev, O. V.; Luponosov, Y. N.; Rempel, A. A.; Valeeva, A. A.;

Stakheev, A. Y.; Turova, O. V.; Mashkovsky, I. S.; Sysolyatin, S. V.; Malykhin, V. V.; Bukhtiyarova, G. A.; Terent'ev, A. O.; Krylov, I. B. *Russ. Chem. Rev.* **2014**, *83*, 885.

(24) Silverstein, R. M.; Webster, F. X.; Kiemle, D. J. *Spectrometric Identification of Organic Compounds*, 7th ed.; John Wiley and Sons, Inc.: Hoboken, NJ, 2005.

(25) Poulton, J. T.; Sigalas, M. P.; Eisenstein, O.; Caulton, K. G. *Inorg. Chem.* **1993**, *32*, 5490.

(26) Feng, Y.; Lail, M.; Barakat, K. A.; Cundari, T. R.; Gunnoe, T. B.; Petersen, J. L. *J. Am. Chem. Soc.* **2005**, *127*, 14174.

(27) (a) Kloek, S. M.; Heinekey, D. M.; Goldberg, K. I. *Angew. Chem., Int. Ed.* **2007**, *46*, 4736. (b) Hanson, S. K.; Heinekey, D. M.; Goldberg, K. I. *Organometallics* **2008**, *27*, 1454.

(28) Bercaw, J. E.; Hazari, N.; Labinger, J. A. *Organometallics* **2009**, *28*, 5489.

(29) Hoyt, H. M.; Bergman, R. G. *Angew. Chem., Int. Ed.* **2007**, *46*, 5580.

(30) Gómez-Gallego, M.; Sierra, M. A. *Chem. Rev.* **2011**, *111*, 4857.

(31) (a) Fulton, J. R.; Sklenak, S.; Bouwkamp, M. W.; Bergman, R. G. *J. Am. Chem. Soc.* **2002**, *124*, 4722. (b) Conner, D.; Jayaprakash, K. N.; Wells, M. B.; Manzer, S.; Gunnoe, T. B.; Boyle, P. D. *Inorg. Chem.* **2003**, *42*, 4759. (c) Fox, D. J.; Bergman, R. G. *Organometallics* **2004**, *23*, 1656.

(32) (a) Blum, O.; Milstein, D. *J. Am. Chem. Soc.* **1995**, *117*, 4582. (b) Blum, O.; Milstein, D. *J. Organomet. Chem.* **2000**, *593−594*, 479. (c) Fafard, C. M.; Ozerov, O. V. *Inorg. Chim. Acta* **2007**, *360*, 286. (d) Fulmer, G. R.; Muller, R. P.; Kemp, R. A.; Goldberg, K. I. *J. Am. Chem. Soc.* **2009**, *131*, 1346. (e) Smythe, N. A.; Grice, K. A.; Williams, B. S.; Goldberg, K. I. *Organometallics* **2009**, *28*, 277.

(33) Somorjai, G. A.; Li, Y. *Introduction to Surface Chemistry and Catalysis*;, 2nd ed.; John Wiley and Sons, Inc.: Hoboken, NJ, 2010.

(34) Grotjahn, D. B. In *Comprehensive Organometallic Chemistry II*; Stone, F. G. A., Wilkinson, G., Eds.; Elsevier: Oxford, 1995; p 741.

(35) (a) Lamata, M. P.; San José, E.; Carmona, D.; Lahoz, F. J.; Atencio, R.; Oro, L. A. *Organometallics* **1996**, *15*, 4852. (b) Saito, S.; Yamamoto, Y. *Chem. Rev.* **2000**, *100*, 2901.

(36) (a) Wakatsuki, Y.; Yamazaki, H.; Kumegawa, N.; Satoh, T.; Satoh, J. Y. *J. Am. Chem. Soc.* **1991**, *113*, 9604. (b) Bianchini, C.; Frediani, P.; Masi, D.; Peruzzini, M.; Zanobini, F. *Organometallics* **1994**, *13*, 4616. (c) Straub, T.; Haskel, A.; Eisen, M. S. *J. Am. Chem. Soc.* **1995**, *117*, 6364.

(37) (a) Lewis, R. A.; George, S. P.; Chapovetsky, A.; Wu, G.; Figueroa, J. S.; Hayton, T. W. *Chem. Commun.* **2013**, *49*, 2888. (b) Zhang, L.; Liu, Y.; Deng, L. *J. Am. Chem. Soc.* **2014**, *136*, 15525. (c) Zolnhofer, E. M.; Käß, M.; Khusniyarov, M. M.; Heinemann, F. W.; Maron, L.; van Gastel, M.; Bill, E.; Meyer, K. *J. Am. Chem. Soc.* **2014**, *136*, 15072.

(38) Halpern, J. *Acc. Chem. Res.* **1970**, *3*, 386.

(39) Burgess, S. A.; Devarajan, D.; Bolaño, T.; Ess, D. H.; Gunnoe, T. B.; Sabat, M.; Myers, W. H. *Inorg. Chem.* **2014**, *53*, 5328.

(40) Fulmer, G. R.; Herndon, A. N.; Kaminsky, W.; Kemp, R. A.; Goldberg, K. I. *J. Am. Chem. Soc.* **2011**, *133*, 17713.

(41) Böhler, C.; Avarvari, N.; Schönberg, H.; Wörle, M.; Rüegger, H.; Grützmacher, H. *Helv. Chim. Acta* **2001**, *84*, 3127.

(42) Goeden, G. V.; Caulton, K. G. *J. Am. Chem. Soc.* **1981**, *103*, 7354.

(43) (a) Rascón, F.; Wischert, R.; Copéret, C. *Chem. Sci.* **2011**, *2*, 1449. (b) Wischert, R.; Laurent, P.; Copéret, C.; Delbecq, F.; Sautet, P. *J. Am. Chem. Soc.* **2012**, *134*, 14430. (c) Copéret, C.; Estes, D. P.; Larmier, K.; Searles, K. *Chem. Rev.* **2016**, *116*, 8463.

(44) (a) Mayer, J. M. *Acc. Chem. Res.* **1998**, *31*, 441. (b) Borovik, A. S. *Chem. Soc. Rev.* **2011**, *40*, 1870. (c) Dietl, N.; Schlangen, M.; Schwarz, H. *Angew. Chem., Int. Ed.* **2012**, *51*, 5544. (d) Liu, W.; Groves, J. T. *Acc. Chem. Res.* **2015**, *48*, 1727.

(45) (a) Kopinke, F. D.; Zimmermann, G.; Anders, K. *J. Org. Chem.* **1989**, *54*, 3571. (b) Blanksby, S. J.; Ellison, G. B. *Acc. Chem. Res.* **2003**, *36*, 255. Marcus theory suggests that at 823 K the tertiary C−H bond in isobutane (96.5 kcal/mol) should react about twice as fast as the secondary one in propane (98.6 kcal/mol) (ignoring differences in the self exchange rate constants). This matches observations from experimental H• transfer rates quite well, as shown in reference 45a. However, since propane has two secondary C−H bonds versus the one

tertiary C—H bond in isobutane, propane and isobutane would be expected to have approximately the same TOF.

(46) Kerr, J. A.; Trotman-Dickenson, A. F. *Trans. Faraday Soc.* **1959**, *55*, 572.

(47) (a) Bunel, E.; Burger, B. J.; Bercaw, J. E. *J. Am. Chem. Soc.* **1988**, *110*, 976. (b) Thieuleux, C.; Maraval, A.; Veyre, L.; Copéret, C.; Soulivong, D.; Basset, J.-M.; Sunley, G. J. *Angew. Chem., Int. Ed.* **2007**, *46*, 2288. (c) Norsic, S.; Larabi, C.; Delgado, M.; Garron, A.; de Mallmann, A.; Santini, C.; Szeto, K. C.; Basset, J.-M.; Taoufik, M. *Catal. Sci. Technol.* **2012**, *2*, 215. (d) Zhugralin, A. R.; Kobylianskii, I. J.; Chen, P. *Organometallics* **2015**, *34*, 1301. (e) O'Reilly, M. E.; Dutta, S.; Veige, A. S. *Chem. Rev.* **2016**, *116*, 8105.

(48) Vogt, E. T. C.; Weckhuysen, B. M. *Chem. Soc. Rev.* **2015**, *44*, 7342.